

DESIGN PARAMETERS FOR RETROFITTED MASONRY TO TIMBER CONNECTIONS

Susana Moreira¹, Luís F. Ramos¹, Daniel V. Oliveira¹ and Paulo B. Lourenço¹

¹ ISISE, Department of Civil Engineering, University of Minho
Campus de Azurém, 4800-058 Guimarães, Portugal
{smoreira, lramos, danvco, pbl}@civil.uminho.pt

Keywords: connections, wall-to-floor, wall-to-timber framed wall, injection anchors, cyclic pullout, backbone curve, acceptance criteria

Abstract. *Proper structural connections play an important role in ensuring seismic loads distribution and developing global damage mechanisms of structures. In unreinforced masonry buildings, positive connections between masonry walls and timber floors or walls through the use of anchors can prevent the occurrence of out-of-plane mechanisms and promote box-behavior. Therefore, this paper aims at developing structural modeling parameters and acceptance criteria that allow the design of anchored connections for historical URM buildings from the late 19th century, in Portugal. An experimental campaign was carried out, where quasi-static monotonic and cyclic pullout tests were carried out on strengthened wall-to-floor connections and wall-to-timber framed connections. Both retrofitting solutions rely on anchoring the timber floor or framed wall to the masonry wall, through the use of steel tie-rods with anchor plates or injection anchors, respectively. From these tests, it was possible to study their hysteretic behavior and failure modes, as well as quantify the maximum pullout capacity, the ductility, the energy dissipation and other parameters. This information was the base to establish multilinear backbone curves and design parameters for each type of behavior observed experimentally. Experiments performed in strengthened wall-to-floor connections with two wall thicknesses (0,4 m and 0,6 m) and in wall-to-timber framed wall connections with injection anchors at the top of a wall demonstrated high ductility and were classified as deformation-controlled actions. Being governed by shear slip enabled them to obtain large displacements with small strength loss. For the injection anchors, the applicability of strength prediction formulas based on different failure models was studied. The adapted ACI 530-05 model for cone breakout was the one that better predicted the experimental values obtained for the tests performed at the top of the wall. Bond failure models were highly dependent on the bond strength of the grout/masonry interface and provided reasonable approximation to the results. Further use requires the determination of accurate grout/masonry interface bond strength. Future work includes simplification of backbone curves and development of hysteretic rules.*

1 INTRODUCTION

The seismic vulnerability of unreinforced masonry (URM) buildings is well recognized in literature [1], as well as the importance of the connections between the primordial structural components, the masonry walls and the timber floors or walls [2; 3]. Even if the importance of their presence has been recognized for a long time as vital in developing appropriate box-behavior and global damage mechanisms, the topic has been “neglected” over time. It is difficult to collect information about masonry-to-timber connections because usually they are not at sight on the finished building and blueprints of old URM buildings are not available. On post-earthquake surveys, due to safety issues, assessment is conducted from outside the URM buildings, so no information is retrieved about the conditions of the connections and the timber diaphragm [1]. To act on the conservation of historical buildings, it is of pressing importance to study the behavior of structural connections and to develop appropriate and engineered retrofitting solutions.

Since few works have been carried out on the topic [4; 5], it was necessary to start from scratch with an experimental campaign, which provided the much needed information to develop structural modeling parameters and acceptance criteria. Two configuration of connections – wall-to-floor and wall-to-timber framed wall – were chosen as base of the experimental campaign and following analysis, to be carried out under the European program NIKER (New integrated Knowledge based approaches to the protection of cultural heritage from Earthquake-induced Risk) and in collaboration with the contractor Monumenta Ltd. Construction details, materials and loading conditions of the specimens meant to replicate connections found in two typologies of URM buildings built during the 19th century, in Portugal (*Pombalino Tardio* and *Gaioleiro*), which are recognized for their seismic vulnerability.

Using the data obtained from cyclic pullout tests, this paper aims at developing backbone curves for each type of connection and acceptance criteria so that they can be integrated in nonlinear numerical analysis of whole structures and better describe their behavior. The approach used to establish the design parameters was based on the ASCE/SEI 41-06 guidelines [6].

For the injection anchors applied in wall-to-timber framed wall connections, was studied the applicability of different strength prediction formulas, based on distinct failure models, to the experimental results. In this way, is possible to understand the impact of different parameters in the performance of the anchors, and take the first steps towards a more generalized use of the prediction formulas.

2 EXPERIMENTAL CAMPAIGN

2.1 Test set-up

The experimental campaign consisted of twenty four pullout tests of wall-to-floor (17 tests) and wall-to-timber framed wall (7 tests) connections. Since the experimental behavior was analyzed in previous papers [7; 8], a summary of the setup is presented in this paper. Both types of specimens included a rubble masonry wall as primary component. These walls were hand constructed by professional masons, and are constituted by limestone of different sizes (maximum dimension of 0.20 m) with poor mortar joints, at most 0.05 m thick. Walls were 2.0 m long, 1.6 m high, and thickness was 0.4 m or 0.6 m. Walls of wall-to-timber framed wall specimens were all 0.4 m thick.

Specimens representing wall-to-floor connections had a timber floor joist with a cross-section of $0.13 \times 0.18 \text{ m}^2$, placed perpendicularly to the wall and nailed to a timber wall-plate of $0.095 \times 0.095 \times 1.000 \text{ m}^2$ built in along the wall (*frechal*). The timber floor joist went 0.15 m into the wall, while the wall-plate was placed 0.03 m from the inner face of the wall. Each wall had two sets of timber floor joists and wall-plates, therefore two pullout tests per wall were performed. The strengthening solution was developed in cooperation with the company Monumenta Lda. and consisted of a steel angle bolted to the floor joist, anchored to the wall by a tie rod with a squared anchor plate. On each end of the tie rod there was a stainless steel half-sphere in a cup, which was intended to work as a hinge (see Figure 1a). The steel angle, half-sphere and cup shapes and dimensions are part of the specificities of this solution. The tie rod was in 8.8 grade steel, had a $\phi 16$ diameter and was applied at a 15° angle. The anchor plate was squared, with the dimensions of $0.175 \times 0.175 \times 0.020 \text{ m}^3$ for 0.60 m thick walls and $0.175 \times 0.175 \times 0.006 \text{ m}^3$ for the 0.40 m thick walls.

For wall-to-timber framed wall connections, in the less conservative typology, the timber framed wall has no intermediate connections with the wall along its height, being connection ensured by the floor joists at top and bottom. In historical buildings, is also common to find degraded timber elements inside the wall, usually with decreased sections, due to humidity damage. Therefore, it was defined that no timber elements would be included in the specimens, and only the anchoring system would be studied. The injection anchors were placed in pairs, in pre-drilled holes of 50 mm, spaced of 280 mm, considering that a 120 mm thick timber framed wall could fit between them (see Figure 2a). The steel ties that are part of the anchors were in stainless steel AISI 304 class 70, and had a diameter of $\phi 20$ (wall 1) and $\phi 16$ (wall 2).

As shown in Figure 1 and Figure 2, the expected failure modes are: masonry cone breakout (FM1), crushing of the masonry under the anchor plate (FM2), failure of the bolted connection between the steel angle and the timber floor joist (FM3), yielding of the steel tie (FM4), sliding at the interface grout/masonry (FM5) and sliding at the interface steel tie/grout (FM6). FM3 is a very complex failure mode because is the result of combined effects that occur at the bolted connection. It comprises crushing of the timber floor joist, bending and shear failure of the bolts, and yielding of the steel angle.

Considering laboratory limitations in terms of space as well as the size of specimens, it was possible to develop a self-balanced test apparatus capable of redirecting the pullout force back to the specimen, as shown in Figure 1 and Figure 2. In order to simulate the compression state of the walls resulting from permanent loads, four hydraulic cylinders were placed over rigid steel profiles on top of the walls. Since the application of the strengthening until testing, the compression state was kept constant through manual control of the pressure. The compression stresses of 0.2 MPa and 0.4 MPa, correspond respectively to the thicknesses of 0.4 m and 0.6 m.

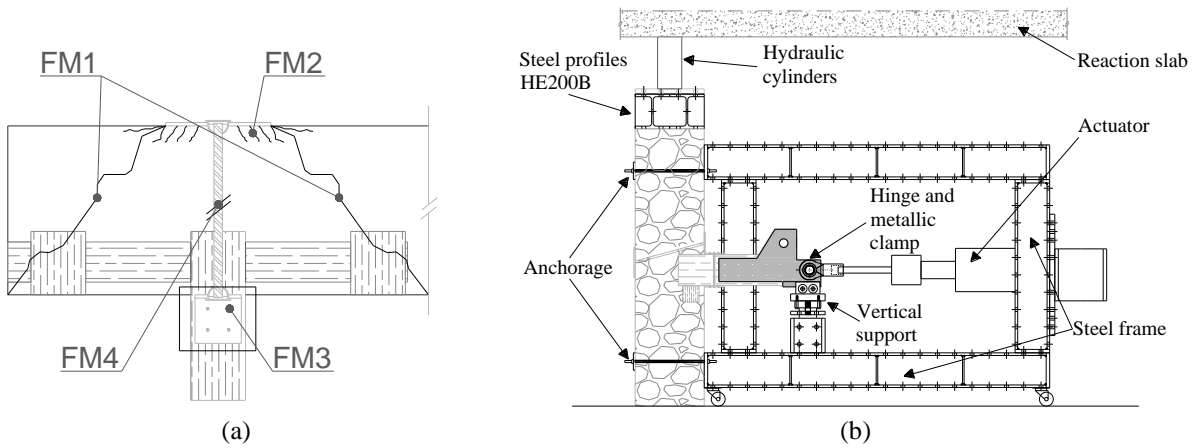


Figure 1: Wall-to-floor pullout: (a) failure modes; and (b) test apparatus.

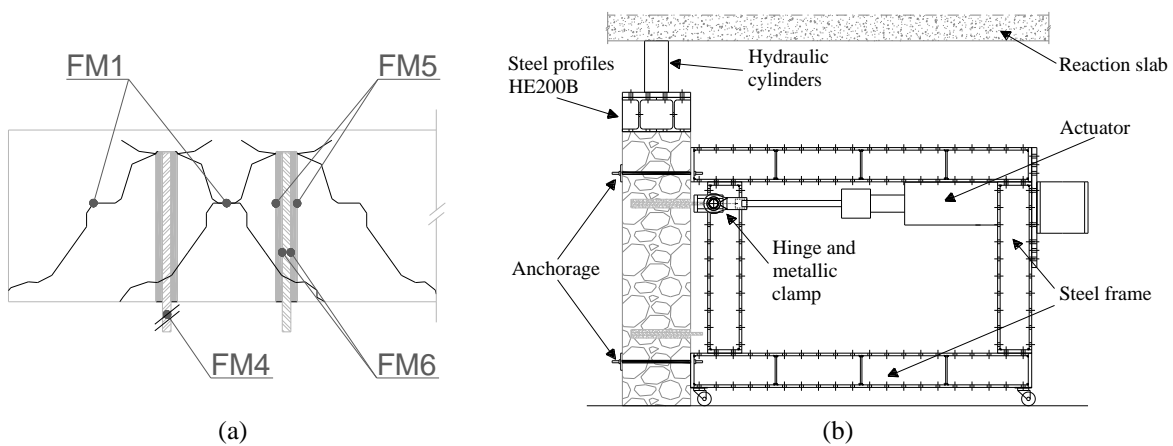


Figure 2: Wall-to-timber framed wall pullout: (a) failure modes; and (b) test apparatus.

2.2 Results

2.2.1. Wall-to-floor connections

The main results of the eight quasi-static cyclic tests on strengthened wall to floor connections are presented in Table 1. The average values of the pullout forces of the two thicknesses of walls are very close, being the one of the 0,4 m walls slightly higher, contrary to what was expected. This is possibly due to the fact that for the 0,6 m walls the masonry cone breakout did not occur. For the 0,4 m walls, failure in all specimens resulted from the combination of masonry cone breakout with failure of the bolted connection (FM1 + FM3), resulting in great similarity of the hysteresis loops [8]. The 0,6 m walls presented mainly failure modes FM3 and FM4 but with similar hysteresis loops until failure. Specimens WF.60.A.3 and WF.60.A.4B had brittle failure modes, bending of the wood joist at the bolted connection, which broke completely, and failure of the steel rod. Specimens WF.60.A.2B and WF.60.A.3B failed by ripping of the wood joist at the bolted connection. Due to the variety in failure modes, the 0,6 m walls presented higher Coefficients of Variation (CoV) than the ones obtained for the 0,4 m walls (below 10%).

The yield displacement (Δ_y), and the ultimate displacement (Δ_u) of the strengthening connection were estimated based on the joist/wall slip, which is the relative displacement between the timber floor joist and the front face of the wall. The yield displacement was taken as the displacement when first yielding occurs, and the ultimate displacement corresponded to

the displacement at the 100 mm step, for the 0,4 m walls, and to the post-peak displacement when a loss of 20% load carrying capacity happened [9], for the 0,6 m walls. In spite of this last criterion being more common, it was not possible to apply it to the 0,4 m walls because the required load carrying capacity loss was not obtained. The ratio between Δ_u and Δ_y is the displacement ductility factor, μ , which expresses the energy dissipation capacity of the strengthened connection. The displacement ductility determined for the 0,4 m walls is extremely high, because the connection is governed by shear slip, creating a plateau after yielding (see Figure 3a). For the 0,6 m walls, the strengthened connection also displays ductility factors characteristic of ductile components.

Table 1 Parameters resultant from the experimental campaign on wall-to-floor strengthened connections

Specimen	F (kN)	Δ_y (mm)	Δ_u (mm)	μ
40.3A	93,09	0,98	91,47	93,71
40.3B	105,38	-	-	-
40.4A	94,50	0,80	84,32	105,90
40.4B	94,07	0,93	88,04	95,03
Average	96,8	0,9	87,9	98,2
CoV (%)	5,2	8,4	3,3	5,6
60.2B	92,42	2,97	74,59	25,11
60.3A	82,67	2,61	41,18	15,76
60.3B	100,65	4,59	107,78	23,47
60.4B	90,02	2,26	59,19	26,19
Average	91,4	3,1	70,7	22,6
CoV (%)	7,0	28,7	34,6	18,0

The similarity in force-displacement curves, especially during the pre-peak, occurs because the connections were governed by the single shear bolted connection between the timber joist and the steel angle. These mechanisms are crushing of the timber joist and shear failure of the bolts. The hysteretic behavior encloses loss of strength between cycles, stiffness degradation and pinching (see Figure 3). As one can see, compression forces associated with reversing the cycle are small, as result of the imposed test procedure. In all tests, there is a loss of force in the range of 20 kN to 70 kN because of the detachment of the steel angle from the timber joist. Tests from both 0,4 m and 0,6 m walls, dissipated most of their energy through the ripping of the wood joists, consequently there is not a big difference between them [8].

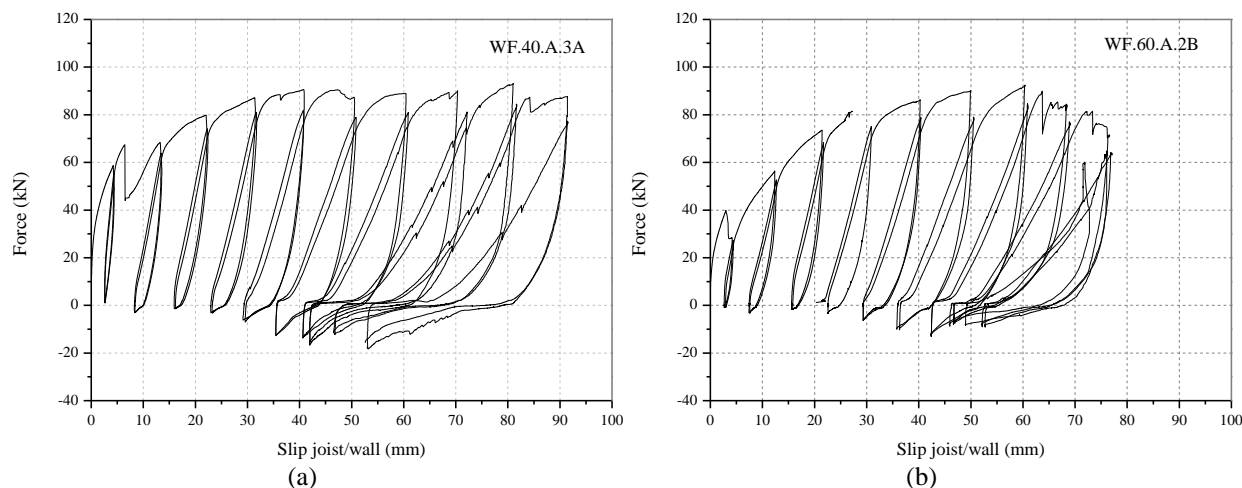


Figure 3 Typical pullout force-displacement curves for wall-to-floor connections: (a) 0.4 m thick wall; and (b) 0.6 m thick wall.

2.2.2. Wall-to-timber framed wall connections

The main results of the five quasi-static cyclic tests on strengthened wall-to-timber framed wall connections are presented in Table 2. There is a significant difference, approximately 30%, in the maximum pullout force between tests conducted at the top and the bottom of the wall. At the base of the wall the average maximum pullout force was 107.9 kN, while at the top the same parameter reached 76.8 kN, both with a CoV below 5%.

The ultimate displacement was calculated in the same way as for the tests performed on wall-to-floor connections with a 0,6 m thick wall. Both yielding and ultimate displacements were obtained from the total slip (s_T), which is the relative displacement between the loaded end of the anchors and the back face of the wall. Specimens at the bottom of the wall have a smaller ductility factor than the ones at the top. The ductility factor determined for specimen WT.40.I.1D was very high when compared to the other specimens, probably due a different arrangement of the masonry and of the interface grout/masonry.

Table 2 Parameters resultant from the experimental campaign on wall-to-timber framed wall strengthened connections

Specimen	F (kN)	Δ_y (mm)	Δ_u (mm)	μ
WT.40.I.1A	111,7	2,5	6,8	2,7
WT.40.I.2A	107,2	-	-	-
WT.40.I.2B	104,9	2,7	9,5	3,5
Bottom average	107,9	2,6	8,2	3,1
CoV (%)	3,2	5,4	23,6	18,3
WT.40.I.1D	81,2	0,7	12,1	18,6
WT.40.I.2C	75,0	0,9	6,7	7,4
Top average	76,8	1,5	10,8	9,4
CoV (%)	4,0	74,5	42,7	66,7

Force-displacement hysteresis loops of specimens WT.40.I.1A and WT40.I.2C represent the typical curves of tests performed at the bottom and top of the wall, respectively (see Figure 4). As can be observed, the pinched hysteresis loops show great similarity, and are

controlled by bond slip phenomena at the grout/masonry interface. The cyclic behavior shows a degradation of force and stiffness with the increasing steps and an accumulation of residual displacements. The descending branches of the cycles pushed the specimen as much as 0.5 mm, which caused the development of compressive forces. The values of this force obtained for top and bottom of the walls were very close (21.0 kN and 23.9 kN), not portraying the clear distinction noticed for tension. Residual displacements and compression forces depend greatly on the composition of the interface grout/masonry and surrounding masonry.

All tests showed combined cone-bond failure with sliding at the interface grout/masonry and masonry breakout. Tests at the top showed a higher influence of the masonry cone while tests at the bottom showed bond failure at the interface grout/masonry as the major contributor for failure.

Differences between tests performed at the top and bottom of the wall are probably due to distinct boundary conditions. Lower out-of-plane displacements of the walls, higher pullout force, lower ductility and shape of the force-displacement curves support the explanation that the bottom of the wall behaves like a fixed support, while the top resembles a pinned support.

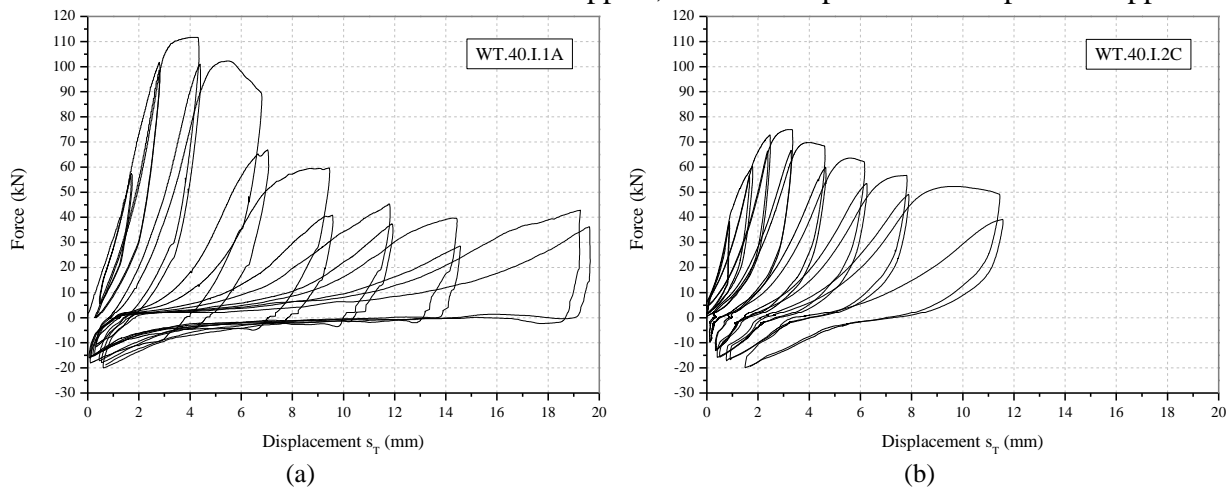


Figure 4 Typical pullout force-displacement curves for injection anchors: (a) bottom of the wall; and (b) top of the wall.

3 DESIGN PARAMETERS

3.1 Backbone curves

Since there are not common standard procedures to design connections, the experimental data collected allowed the possibility to define modeling parameters and acceptance criteria according to ASCE/SEI 41-06 [6]. As described, the test set-up attempted to replicate, as much as possible, the historical construction details, the materials, the boundary conditions, and the stress state of the walls, as expected in real buildings. Due to test set-up limitations, the cyclic loading was not fully reversed, tension and compression. In compression, it can be assumed that the connection will be governed by out-of-plane behavior of the wall but further analysis needs to be performed.

A backbone curve is an idealized multi-linear force-displacement pushover curve, derived from several experiments and intends at being used for structural modeling. As prescribed in the ASCE/SEI 41-06 [6], for each specimen, a smooth backbone was defined by the intersections between the first cycle curve for the i -th deformation step with the second cycle curve of the $(i-1)$ th deformation step, for all i steps. Then, each curve was converted into several linear segments, and after averaged into a single multilinear representation of the

connections, as presented in Figure 5 and Figure 6. Further work needs to be developed in decreasing the number of linear segments, into 3 or 4, so that implementation becomes easier. To do so, further analysis of the dissipated energy needs to be developed.

Next step consisted of determining which type of action controls each kind of connection, force or deformation. Being connections primary components, in order to be considered deformation controlled, need to have a displacement at the end of the strain-hardening of softening branch higher than two times the displacement at yielding. This condition was verified for both strengthened wall-to-floor connections (0,4 m and 0,6 m), and for strengthened wall-to-timber framed wall connections at the top of the wall (see Figure 5 and Figure 6a), being then classified as having a ductile behavior. For the average backbone curve of the 0,6 m thick wall connections, specimen WF.60.3A was not considered due to its premature failing. The backbone curve of the strengthened wall-to-timber framed wall connection performed at the bottom of the wall is force-controlled.

Points 1, 2 and 3 regard limits of distinct phases of the behavior of the connection. The elastic phase goes from 0 to 1, the strain hardening is comprehended between 1 and 2, and the strength degradation phase develops between 2 and 3 (see Figure 5 and Figure 6).

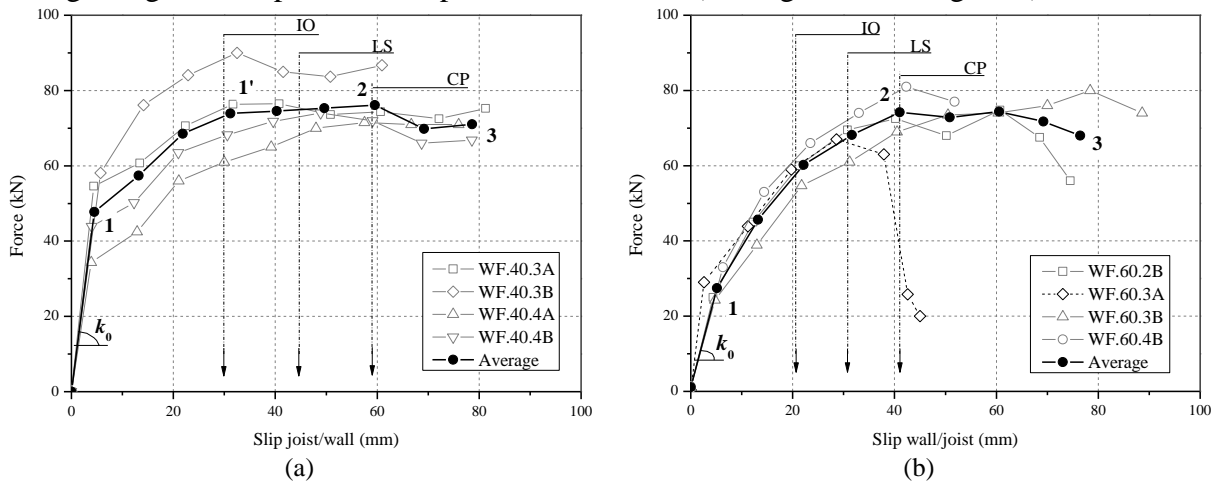


Figure 5 Backbone curves for the strengthened wall-to-floor connections: (a) 0.4 m thick wall; and (b) 0.6 m thick wall.

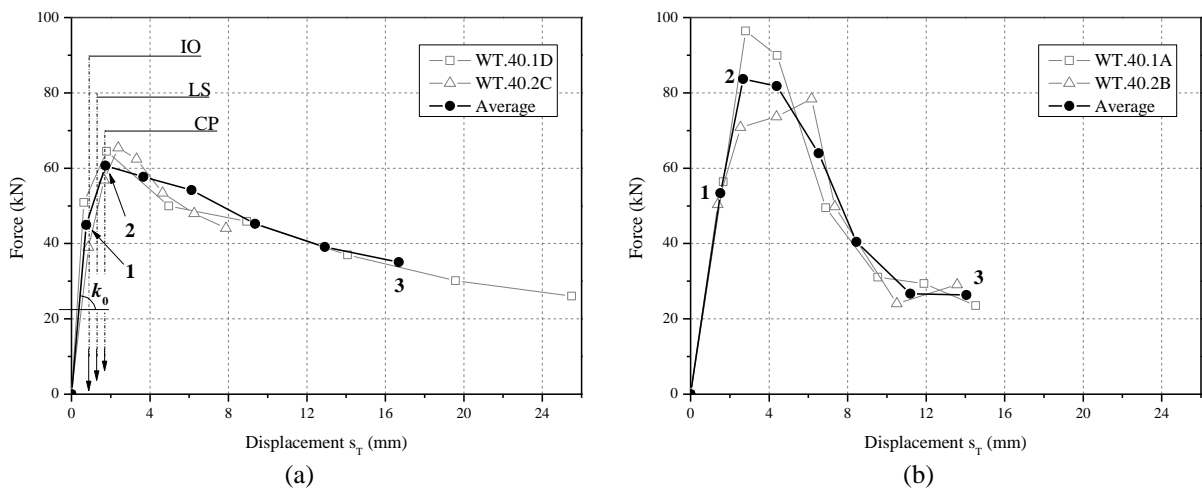


Figure 6 Backbone curves for strengthened wall-to-timber framed wall connections: (a) top wall; and (b) bottom wall.

For the deformation-controlled actions is possible to establish acceptance criteria to use in linear and nonlinear procedures, as represented in Figure 5 and Figure 6a. Deformation, m -factors and expected strength (Q_{CE}) for each level – Immediate Occupancy (IO), Life Safety (LS) and Collapse Prevention (CP) – were calculated and are presented in Table 3. m -factors are modification factors that account for the expected ductility associated with the action and Q_{CE} is the expected strength of the component at the deformation level under consideration. Linear stiffness, k_0 , was determined for the linear branch connecting the origin with point 1.

Table 3 Design parameters and acceptance criteria

	k_0 (kN/mm)	IO			LS			CP		
		Δ_{IO} (mm)	Q_{CE} (kN)	m	Δ_{LS} (mm)	Q_{CE} (kN)	m	Δ_{CP} (mm)	Q_{CE} (kN)	m
WT-Top	60,0	0,9	46,9	0,9	1,3	53,8	1,3	1,7	60,7	1,7
WF.40	10,6	29,9	60,9	5,0	44,7	68,5	7,4	59,0	75,8	9,8
WF.60	5,3	20,6	47,6	3,0	30,8	60,8	4,5	41,0	74,2	6,0

3.2 Strength prediction formulas for injection anchors

The installation and design of anchors in concrete has been widely studied when compared to their use in masonry. As quasi-brittle materials, there are some similarities in behavior that can be explored and contribute to the study of anchors in masonry.

Bonded anchors mainly take advantage of bond and mechanical interlock. The presence of a head on the anchor changes the load transfer mechanisms and has direct consequences on the failure modes. The most common failure modes for unheaded anchors are bond failure at rod/grout interface and bond failure at grout/substrate (concrete or masonry) interface. The existence of the head prevents the failure at the rod/grout interface and adds two more possible failure modes: substrate cone breakout and combined cone-bond failure, as expected for the injection anchors. Headed or not, bonded anchors can also fail by yielding of the steel rod, which can be controlled by properly choosing the steel grade and diameter [10; 11].

Since the mid-1970s, different design methods have been developed to describe concrete cone breakout, based initially on plasticity models (modified Coulomb failure condition), and later on, on linear elastic fracture mechanics (LEFM) [12]. In Table 4, the approaches of Cook et al. [11] and ACI 530-05 [13] are based on the plasticity method, therefore they assume the maximum tensile stress uniformly distributed on the projected area of a 45° angle stress cone radiating from the free end of the anchor towards the loaded end. On the other hand, Zamora et al. [10] idealized the cone breakout stress projection as being a 35° angle pyramid and related the tensile capacity with fracture toughness ($k_c = 11.6$ in Equation (2), for concrete). The ψ -factors account for geometric alterations on the projection area $A_{p,N}/A_{p,N}^0$ (free edge, spacing between anchors, etc.), the influence of edges of the concrete member on the distribution of stresses in the concrete ($\psi_{s,N}$), and for the group effect when different tension loads are imposed to the individual anchors of a group ($\psi_{ec,N}$).

Bond failure depends on the embedment length, h_e , the pre-drilled hole diameter, d_0 , or the steel rod diameter d and the nominal bond strengths – τ' or τ'_0 – depending on which interface is being considered, grout/masonry or steel rod/grout, respectively. The combined cone-bond failure model is the sum of the contributions of cone failure and bond failure, and requires the calculation of a shallow cone depth (h_c), which determines the extent of each one of them.

The ACI 530-05 estimates the value of the tensile strength of brick masonry by using the expression $0.33\sqrt{f'_m}$, where f'_m is the nominal compressive strength of masonry. The other two parameters are the effective embedment length l_b and the factor that accounts for superposition of projection areas $A_{p,N}/A_{p,N}^0$.

All equations presented in Table 4 are expressed in SI units (N, mm, and N/mm²).

Table 4 Tensile force prediction formula for a group of anchors

Method	Application	Formula
Cook et al. (1998) [11]	Combined cone-bond failure of adhesive anchors for concrete	$\frac{A_{p,N}}{A_{p,N}^0} 0.85 h_c^2 \sqrt{f_{cc,200}} + \frac{A_{p,N}}{A_{p,N}^0} \pi \tau d (h_e - h_c)$ <p style="text-align: right;">(1)</p> <p style="text-align: center;">, if $h_e > h_c$ and $h_c = \frac{\tau \pi d}{2\sqrt{f_{cc,200}}}$</p>
Zamora et al. (2003) [10]	Cone failure of grouted anchors for concrete	$\frac{A_{p,N}}{A_{p,N}^0} \psi_{s,N} \psi_{ec,N} 11.6 \sqrt{f'_{cc,200}} h_e^{1.5}$ <p style="text-align: right;">(2)</p>
Zamora et al. (2003) [10]	Bond failure of single grouted anchor in concrete	$\frac{A_{p,N}}{A_{p,N}^0} \tau'_0 \pi d_0 h_e$ <p style="text-align: right;">(3)</p>
ACI 530-05 [13]	Cone failure of headed anchors for brick masonry	$\frac{A_{p,N}}{A_{p,N}^0} 0.33 \pi l_b^2 \sqrt{f'_m}$ <p style="text-align: right;">(4)</p>

When used for design, the previous equations are accompanied by strength-reduction factors, ϕ , which vary with the failure mode. When nominal tensile strength is controlled by steel failure, ϕ is 0.90. For anchor pullout, it should be taken as 0.65 and for masonry breakout is further reduced to 0.50 [13].

A comparison between the experimental results and some of the existing strength prediction formulas for tensile capacity was performed, as presented in Figure 7. The tensile strength of the masonry, if calculated with the expression $0.33\sqrt{f'_m}$ is in this case 0.44 MPa. This value is 3.14 times higher than the average value obtained from the diagonal compression tests performed on masonry wallets representative of the walls' masonry, 0.14 MPa. As one can conclude, the expression used to estimate the tensile strength may be suitable for clay brick and concrete blocks masonry, but doesn't provide a good estimation for rubble stone masonry. Tomazevic [2] suggested the interval of (0.03-0.09) f_m to estimate the tensile strength, where the multiplying factor varies according to the masonry type. For this particular case, the tensile strength (0.14 MPa) corresponds to approximately 0.08 f_m , which falls within the proposed range.

The estimation using the ACI 530-05 code [13] referred as "original" used the value 0.44 MPa for the tensile strength of masonry, the remaining ones used 0.14 MPa. The full length of embedment was assumed as effective, therefore a h_e of 350 mm was considered to estimate the cone failure. In the bond models, the values of 0.53 MPa (minimum) and 1.64 MPa (maximum) were taken for τ_0 , which were determined by Algeri et al. [5] for the interface between cementitious grout and different kinds of limestone.

The tensile capacity for cone failure calculated with the ACI 530-05 [13] formula and 0.44 MPa as the tensile strength of masonry is considerably overestimated, confirming the inadequacy of the expression $f_t = 0.33\sqrt{f'_m}$ for rubble masonry. On the other hand, the adapted formula predicts a tensile strength of approximately 80 kN, which is very close to the value experimentally obtained for the tests at the top of the wall, where the masonry cone failure occurred. As discussed previously, there is a confinement effect of the bottom of the

wall, which probably caused the increase in the tensile strength of the strengthening. This effect should be accounted in the formula by replacing the tensile strength of the masonry with the value of confined tensile strength, f_{ct} , which would be higher than the original.

The cone failure model suggested by Zamora et al. [10] provided a very conservative estimation of the tensile capacity of the strengthening. This model reflects the LEFM approach, which is the most appropriate approach for estimating the tensile capacity but relies on the correct estimation of the factor k_c .

The predictions of the bond models are highly dependent on the bond strength at the interface grout/masonry, reaffirming the necessity of quantifying its value in the product approval. The combined cone-bond model could only be applied with the bond strength of 0.53 MPa ($h_c = 297$ mm), since with 1.64 MPa the h_c is higher than the thickness of the wall ($h_c = 920$ mm $>$ 400 mm). Nevertheless, the model provided a lower value (64 kN) than the values obtained experimentally for the tests performed at the top of the wall but it is a good approximation.

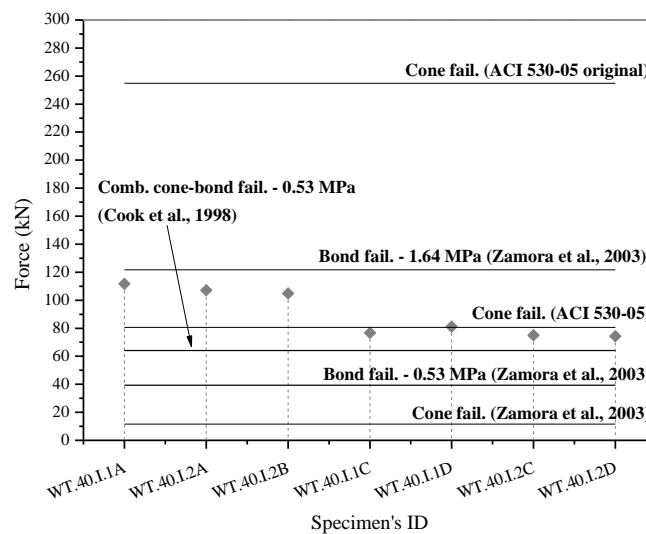


Figure 7 Comparison between strength prediction formulas and the experimental results.

4 CONCLUSIONS

Based on the results of the experimental campaign, it was possible to characterize the cyclic behavior of strengthened wall-to-floor and wall-to-timber framed wall connections, and consequently to derive some design parameters and backbone curves that can be used for linear and nonlinear seismic design.

Strengthened wall-to-floor connections and strengthened wall-to-timber framed wall connections at the top of the wall display a ductile behavior, with high ductility factors and backbone curves classified as deformation-controlled. Further work on these curves, will focus on simplifying the backbone curves and describing loading-unloading rules, taking into consideration energy dissipation, strength and stiffness degradation and pinching. This approach enables performance-based design of the strengthening connections and the consideration of their nonlinear behavior in global structural analysis.

For the injection anchors, the adapted ACI 530-05 [13] model for cone breakout and the combined cone-bond failure model [11] (0,53 MPa) were the ones that better predicted the experimental values obtained for the tests performed at the top of the wall, which is consistent with the failure modes observed. For the tests performed at the bottom of the wall, the best approximation was obtained with the bond failure model of Zamora et al. [10] for a bond strength of 1,64 MPa. The predictions of bond failure models are highly dependent on the

bond strength of the grout/masonry interface, which needs to be properly characterized to improve the accuracy of this type of models.

The first steps towards a better knowledge of the design of strengthened connections were taken successfully but further work needs to be developed in adapting the existent approaches to the connections behavior.

REFERENCES

- [1] M. Bruneau, State-of-the-art report on seismic performance of unreinforced masonry buildings. *Journal of Structural Engineering*, **120**(1), 230–, 1994.
- [2] Tomažević M. Earthquake-resistant design of masonry buildings. Elnashai AS, Dowling PJ, editors. Imperial College Press; 1999.
- [3] R. Bento, M. Lopes & R. Cardoso, Seismic evaluation of old masonry buildings. Part II: Analysis of strengthening solutions for a case study. *Engineering Structures*, **27**(14), 2014–2023, 2005, doi:10.1016/j.engstruct.2005.06.011.
- [4] T. J. Lin, J. M. LaFave, Experimental structural behavior of wall-diaphragm connections for older masonry buildings. *Constr Build Mater.* **26**, 180–9, 2012.
- [5] C. Algeri, E. Poverello, G. Plizzari and E. Giuriani, Experimental study on the injected anchors behaviour on historical masonry. *Advanced Materials Research*, **133-134**, 423-428, 2010.
- [6] ASCE-SEI, Seismic rehabilitation of existing buildings (ASCE/SEI 41-06), 2006.
- [7] S. Moreira, L. F. Ramos, D. V. Oliveira, R. P. Fernandes, J. Guerreiro, P. B. Lourenço, Experimental seismic behavior of wall-to-half-timbered wall connections. *8th International Conference on Structural Analysis of Historical Constructions (SAHC 2012)*, Wroclaw, Poland, October 15-17, 2012.
- [8] S. Moreira, L. F. Ramos, D. V. Oliveira, P. B. Lourenço, L. Mateus, Developing a seismic retrofitting solution for wall-to-floor connections of URM buildings with wood diaphragms. *9th International Masonry Conference (9th IMC)*, Guimarães, Portugal, July 7-9, 2014.
- [9] R. Park, Evaluation of ductility of structures and structural assemblages from laboratory testing. *Bull New Zeal Soc Earthq Eng.*, **22**(2), 155–66, 1989.
- [10] N. A. Zamora, R. C. Cook, R. C. Konz and G. R. Consolazio, Behavior and design of single, headed and unheaded, grouted anchors under tensile load. *ACI Structural Journal*, **100**, 222-230, 2003.
- [11] R. A. Cook, J. Kunz, W. Fuchs and R. C. Konz, Behavior and design of single adhesive anchors under tensile load in uncracked concrete. *ACI Structural Journal*, **95**(1), 9-25, 1998.
- [12] R. Piccinin, R. Ballarini and S. Cattaneo, Linear Elastic Fracture Mechanics Pullout Analysis of Headed Anchors in Stressed Concrete. *Journal of Engineering Mechanics*, pp. 761-768, 2010.
- [13] Masonry Standards Joint Committee, ACI 530-05 - Chapter 3: Strength design of masonry in *Building Code Requirements for Masonry Structures*, pp. 31-32, 2005